Accessing alkyl- and alkenyl-cyclopentanes from Cr-catalysed ethylene oligomerization using 2-phosphinophosphinine ligands

Robert J. Newland,[a] Alana Smith,[a] David M. Smith,[b] Natalie Fey,[c] Martin J. Hanton*,[b] and Stephen M. Mansell*,[a]*

[a] Institute of Chemical Sciences, Heriot-Watt University, Edinburgh, EH14 4AS, UK.

[b] Sasol Technology UK, Ltd., Purdie Building, North Haugh, St Andrews, Fife, KY16 9ST, UK.

[c] School of Chemistry, University of Bristol, Cantock's Close, Bristol, BS8 1TS, UK.

KEYWORDS phosphinine, hybrid ligand, chromium, ethylene oligomerization,

Abstract

Desilylation of the 2-phosphinophosphinine 2-PPh_2-3-Me-6-$SiMe_3$-PC_5H_2 with HCl gave 2-PPh_2-3-Me-PC_5H_3, demonstrating the late-stage modification of this bidentate heterocyclic ligand. Group 6 metal carbonyl complexes of these ligands showed κ^2-binding and very small bite-angles of 65.1 – 68.3°, and also demonstrated that the donor properties of 2-phosphinophosphinines can be tuned readily by the presence of the $SiMe_3$ group which gives a

more π-accepting phosphinine ligand. The properties of 2-phosphinophosphinines were compared to bidentate diphosphorus ligands computationally, contextualizing them in the Ligand Knowledge Base for bidentate P,P donor ligands (LKB-PP) and were found to occupy an area of ligand space adjacent to $Ar_2PN(R)NAr_2$ ligands that have been successfully used in ethylene oligomerization reactions, but with well-separated properties in the second principal component. Testing 2-phosphinophosphinines in Cr-catalyzed ethylene oligomerization reactions showed key differences to standard PNP ligands in that a high proportion of alkyl- and alkenyl-cyclopentanes were formed. This demonstrates that the different donor properties of 2-phosphinophosphinines influence the reactivity of the key 7-membered metallacycle postulated in the metallacyclic reaction mechanism, generating products from isomerization and subsequent ethylene insertion. Alkyl- and alkenyl-cyclopentanes represent new products for the key industrial feedstock ethylene, with the alkenes having potential as new monomers, comonomers or additives for plastics. Computational evaluation of ligand properties and the resulting property maps can play a role in suggesting future ligand developments to change the selectivity of this industrially-relevant system in the pursuit of new products generated from ethylene.

Introduction

Ethylene is a key starting material in the chemical industry[1-2] including in the production of valuable linear α-olefins (LAO).[2] Non-selective processes for the production of LAO, such as the SHOP process,[3] have been complemented by selective processes that can be tuned to exactly match market demand, and industrial processes for ethylene dimerization,[4-5] trimerization[6] and tetramerization[2, 7] have all been commercialised.[7] A metallacyclic mechanism (Scheme 1) has

been generally accepted as the reason for high selectivities to 1-hexene and 1-octene,[5, 8] and it is understanding of this distinctive mechanism that has enabled a step change in performance compared to previous unselective oligomerization processes. Encouraged by these successes, there is continued interest in understanding these processes in more detail as well as developing other selective processes to higher LAO (e.g. C10-C18),[3] and to new products.[9-10] Alkyl- and alkenyl-cyclopentanes have been found to be produced by tetramerization catalysts[11-15] and represent a potential target for optimization, by identifying the factors influencing their production from the key 7-membered metallacycle. Alkenes bearing cyclopentane substituents also represent potential monomers giving access to polyolefins with new properties, and polyethylene waxes / short-chain polymers also have materials applications as well.[12]

Scheme 1. Cr catalysed ethylene oligomerization via metallacyclic intermediates, and formation of alkyl- and alkenyl-cyclopentanes. The formation of co-oligomers is not shown.

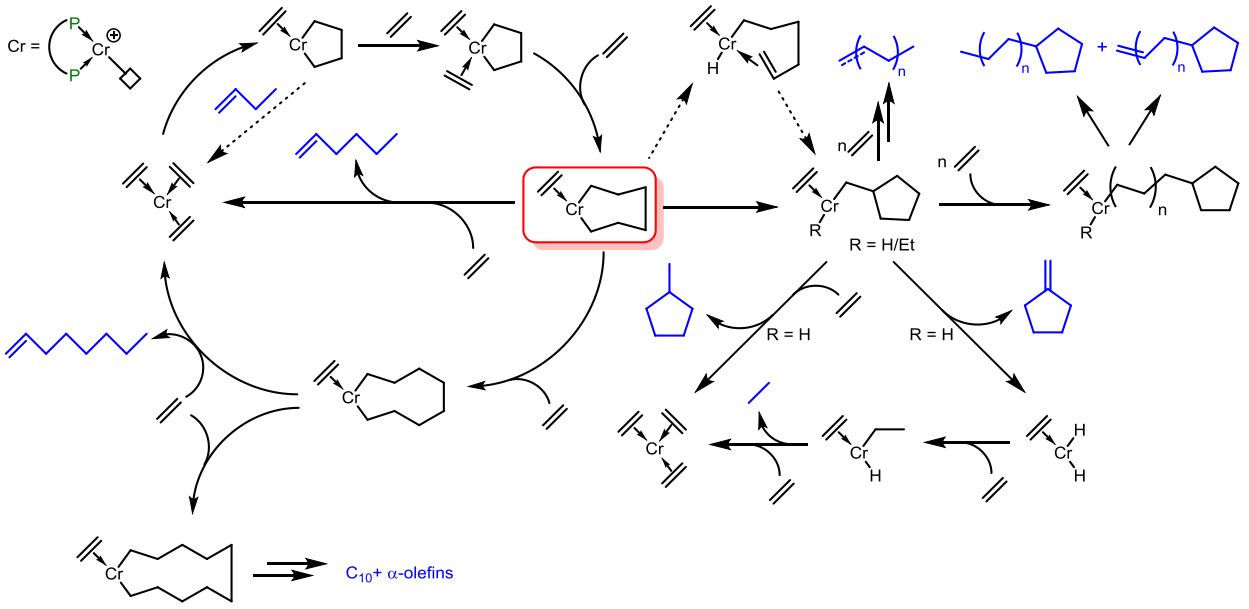

Small bite angle PNP (diphosphinoamine) ligands[16] have proven to be very successful ligands in combination with simple Cr salts and MAO co-activators for selective oligomerization catalysis because they produce highly active catalysts for both trimerization, where they can be extremely selective to 1-hexene (e.g. **A**, Chart 1),[17-18] and for tetramerization (**B**, Chart 1) producing 1-octene in greater than 70% selectivity (along with 1-hexene and other products).[11, 19-20] Although computational and experimental insight into the mechanism has been gained,[9, 11, 13-14, 21-25] definitive spectroscopic identification of the active species in the catalytic cycle has remained out of reach,[26] somewhat hampering catalyst design. When moving from nitrogen to carbon-based ligand backbones, it was established that dppm (**C**, Chart 1, R = H) does not form a selective catalyst, instead generating a Schulz-Flory distribution of LAO,[27] most likely due to deactivation processes involving deprotonation of the acidic methylene group.[27-28] Protection of this position with one alkyl substituent recovered modest catalytic activity and some selectivity for tri- and tetramerization (**C**, R = Me, n-hexyl, benzyl),[28] along with use of ligand **D** which is more resistant to deprotonation,[27] but the unsaturated 1,1-bis(diphenylphosphino)ethene ligand (**E**) gave an unselective catalyst of very low activity.[27] Dppe (**F**, R = H), and related ligands with hydrocarbyl backbones containing unsaturation (**G**, **H**) either with or without backbone substitution, also work well in selective ethylene tetramerization catalysis.[27, 29]

The use of donor-functionalised phosphinines in catalysis is a growing field,[30-34] and incorporation of the ligand backbone and one phosphorus donor in an unsaturated heterocycle, in the form of an aromatic phosphinine,[35] would protect the ligand backbone from deprotonation and give unsymmetrical 2-phosphinophosphinine ligands with potentially very different properties.[32, 35-36] Ligand **1** has recently been used in the Ru catalysed transfer hydrogenation of acetophenones at room temperature as well as the catalytic 'hydrogen borrowing' upgrading of

EtOH/MeOH to ^{i}BuOH.[37] Unsymmetrical ligands are an interesting development in selective oligomerisation catalysis[12, 38] as 1-phosphanyl methanimine ligands (**I**) have recently shown excellent properties in Cr catalysed ethylene oligomerization, achieving conversions of greater than 95% to give high value liquid 1-hexene and 1-octene.[38] In this work, we present a new synthetic route to desilylated 2-phosphinophosphinines, experimentally and computationally characterize the donor properties of 2-phosphinophosphinines, and assess their performance in Cr catalysed ethylene oligomerisation, revealing the formation of alkyl- and alkenyl-cyclopentanes from the key 7-membered metallacyclic intermediate.

Chart 1

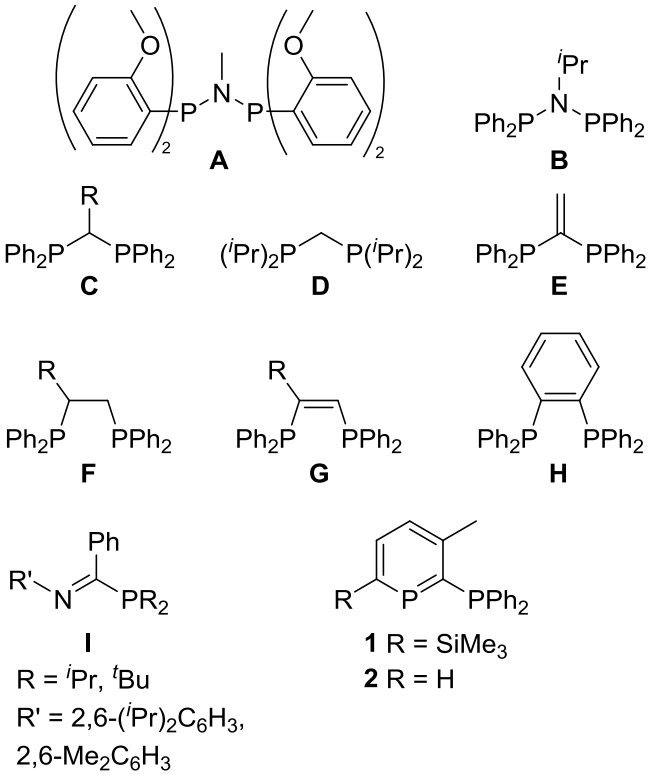

Results and Discussion

Desilylation of 2-PPh_2-3-Me-6-$SiMe_3$-phosphinine

The double protodesilylation of 2,6-bis(trimethylsilyl)phosphinines using ethereal HCl has been shown to be facile when the 3,5 substituents are simple hydrocarbyl groups,[39] and also very recently for 2-trimethylsilylphosphinine.[40] A computational study found that *ortho*-silyl groups should improve both the σ-donating and π-accepting properties of phosphinines,[41] and as the impact of substituent effects on the donor properties of phosphinophosphinine ligands has yet to be investigated, we sought experimental evidence for this hypothesis by comparing the donor properties of ligands **1** and **2**.

Proligand **1** was synthesised as detailed previously from the borane-protected compound **1.BH_3**.[37] Desilylation was achieved both with and without BH_3 protection using one equivalent of HCl in a mixture of Et_2O and CH_2Cl_2 cleanly generating **2.BH_3** or **2** respectively (Scheme 2). ^{31}P NMR spectroscopy showed the phosphinine P resonance at 229.8 ppm in **2.BH_3**, approximately 25 ppm lower than in **1.BH_3** (255.4 ppm),[37] ^1H NMR spectroscopy showed a multiplet resonance at 8.59 ppm for the 6-H in **2.BH_3**, and purity was also established by elemental analysis. **2** has been previously synthesised through a route involving Pd-catalysed cross-coupling of a 2-bromophosphinine.[42] The molecular structure of **2.BH_3** was determined by X-ray diffraction (Figure 1) and showed a planar phosphinine ring bearing a 2-diphenylphosphine substituent bound to BH_3 which is orientated almost perpendicularly to the phosphinine plane (B1-P2-C1-P1 torsion angle is 108.79(13)°). The P-C bond lengths in the ring (1.746(2) and 1.721(2) Å) are shorter than the P-C bond to the PPh_2 moiety (1.822(2) Å), as expected from the aromatic nature of the phosphinine ring, but are noticeably different with P1-

C1 longer by approximately 0.02 Å. The C-C bond lengths in the phosphinine ring fall between 1.380(3) and 1.410(3) Å, typical for those observed in benzene (1.40 Å). Although deprotection of **2.BH$_3$** was achieved with 0.5 equivalents of 1,4-diazabicyclo[2.2.2]octane (DABCO), direct formation of **2** from **1** was preferred due to simpler purification and higher yields.

Scheme 2. Synthesis of proligands and carbonyl complexes. L_2 = NBD (norbornadiene) for Cr and Mo, COD (1,5-cyclooctadiene) for W.

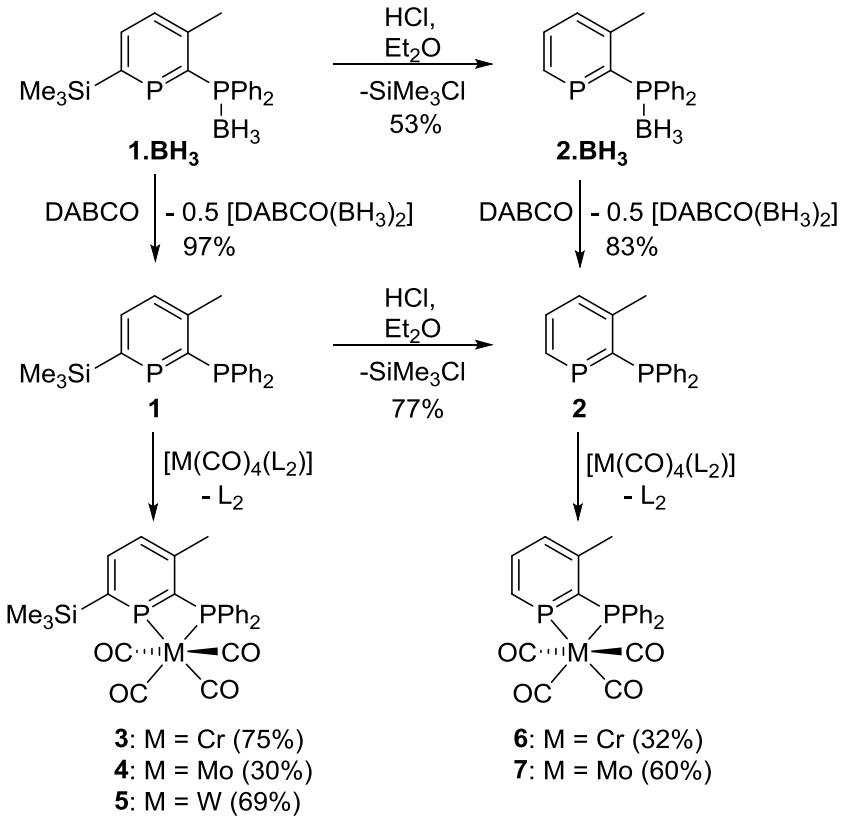

Figure 1. Thermal ellipsoid plot of the molecular structure of **2.BH$_3$** (50% probability).Selected bond lengths (Å) and angles (˚): P2-B1 1.934(3), P1-C1 1.746(2), P1-C5 1.721(2), P2-C1 1.822(2), C1-C2 1.410(3), C2-C3 1.402(3), C3-C4 1.382(3), C4-C5 1.380(3), P1-C1-P2

114.94(12), C5-P1-C1 101.40(11), C2-C1-P1 124.65(16), C3-C2-C1 121.0(2), C4-C5-P1 124.90(17); torsion angle: B1-P2-C1-P1 108.79(13)˚.

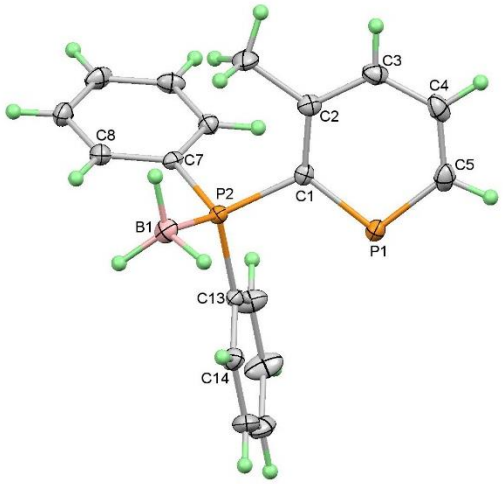

Coordination chemistry

Quantifying ligand properties can help explain experimental observations and guide further catalyst design. Coordination complexes of metal carbonyls have long proven to be a useful means of determining the donor properties of ligands experimentally,[43] such as Tolman's use of $[Ni(L)(CO)_3]$,[44] *trans*-$[Rh(Cl)(L)_2(CO)]$ as a safer alternative[45] or the A_1 vibration in *cis*-$[Mo(CO)_4(L_2)]$ complexes for bidentate ligands.[46] The only previously reported chelating metal carbonyl complex of a 2-phosphinophosphinine is 2-diphenylphosphino-3,4,6-triphenylphosphinine coordinated to $W(CO)_4$, however, only the yield (41%), melting point and observation of the molecular ion by MS were reported.[47] Only bridging complexes of **2** have been reported to date.[48]

1 and **2** react in toluene solution with diene complexes of group 6 tetracarbonyls to generate the corresponding chelating complexes. All compounds were isolated pure after recrystallization

from toluene at low temperature as determined by elemental and spectroscopic analysis. ^{31}P NMR spectroscopic analysis showed two doublets for each complex with $^{2}J_{PP}$ coupling constants that increase in the order proligand (**2**: 31.2 Hz, **1**: 31.6 Hz[37]) < Cr complexes (**3**: 38.2 Hz, **6**: 33.8 Hz) < Mo complexes (**4**: 72.8 Hz, **7**: = 71.1 Hz) < W complex (**5**: 78.0 Hz); **5** also showed additional ^{183}W (I = ½, 14 % abundant) satellites. The phosphinine P chemical shifts are highest for the Cr complexes, with lower frequency resonances for the Mo and W complexes, and the PPh_2 moieties displayed the same pattern. All values for the phosphinine resonances are still typical of P in an aromatic phosphinine environment.[32] $M(CO)_4$ complexes of the chelating 4,5-dimethyl-2-(2-pyridyl)phosphinine ligand are known that show ^{31}P NMR resonances ca. 24 ppm lower for M = Cr and Mo, and ca. 4 ppm lower for W likely due to the different substitution on the phosphinine.[49]

Table 1. Selected analytical data for **1 - 7**.

	1	**2**	**3**	**4**	**5**	**6**	**7**
Phosphinine ^{31}P NMR δ/ppm	249.8	224.9	273.6	244.8	209.6	250.3	222.7
PPh_2 ^{31}P NMR δ/ppm	-7.5	-7.6	40.5	18.9	-0.1	41.8	20.0
$^{2}J_{P\text{-}P}$ / Hz	31.6	31.2	38.2	72.8	78.0	33.8	71.1
$M\text{-}P_{phosphinine}$			2.3752(5)	2.5028(4)	2.4866(6)	2.3464(11)	
$M\text{-}P_{PPh2}$			2.4340(5)	2.5599(4)	2.5462(6)	2.4030(13)	
Bite angle /°			67.99(2)	65.09(1)	65.07(2)	68.29(4)	
P-C-P angle /°	119.9(1)	114.9(1)[a]	97.50(8)	99.98(7)	99.40(11)	97.7(2)	
A_1 CO vibration /cm^{-1}			2013	2026	2021	2003	2017

[a] As determined from the molecular structure of **2.BH$_3$**.

X-ray diffraction experiments on single crystals of **3**, **4** and **5** revealed that they all crystallise in the P-1 space group and are isostructural (Figure 2a, Table S1 and S2). The chelating phosphinophosphinine ligands are bound to distorted octahedral $M(CO)_4$ fragments with P1-C2-P2 angles that are significantly decreased compared to the free ligand (97.50(8)° in **3** to 99.98(7)° in **4** compared to 119.9(1)° in **1**) indicating distortion of the ligand upon coordination. The bite angles are all very small, between: 67.99(2)° in **3** and 65.07(2)° in **5**. In comparison, for $[M(dppm)(CO)_4]$ the bite angles are 70.2° (Cr),[50] 67.3° (Mo)[50] and 67.1° (W).[51] The M-P bond lengths are shorter to the phosphinine P than to the phosphine P (Table 1) as seen previously in a chelating Ru complex.[37] The metal centre is offset compared to the orientation of the phosphinine ring (C3-P1-M1 angle is ca. 151°), emphasising the flexibility of the phosphinine donor in accommodating this geometry, which is likely to be enhanced by the high s-character of the phosphinine lone pair.[32] Single crystal X-ray diffraction experiments on **6** revealed the analogous Cr complex without a $SiMe_3$ group (Figure 2b). The Cr-P bond lengths (Cr-P1 2.3464(11) and Cr-P2 2.4030(13) Å) are ca. 0.03 Å shorter than in **3**, and P1-C5 is also shorter to the analogous distance in **3** by 0.03 Å at 1.705(4) Å, but the bite angle is similar (68.29(4)°). Comparison with (4,5-dimethyl-2-(2-pyridyl)phosphinine)tetracarbonylchromium (Cr-P = 2.280(1) Å)[49] show a longer Cr-phosphinine bond length for **6**. The two crystallographically-characterised Mo-phosphinine complexes show shorter bond lengths of ca. 2.38 Å for $[Mo(PC_5H_5)_6]$[52] and 2.3565(4) Å for a bridging dinuclear complex,[53] and seven crystallographically-characterised W-phosphinine compounds have bond lengths ranging from 2.36 – 2.57 Å.[52, 54-57]

Figure 2. Thermal ellipsoid plot of the molecular structure of **3** (left, **4** and **5** are isostructural) and **6** (right). Thermal ellipoids are at 50% probability and hydrogen atoms are omitted for clarity.

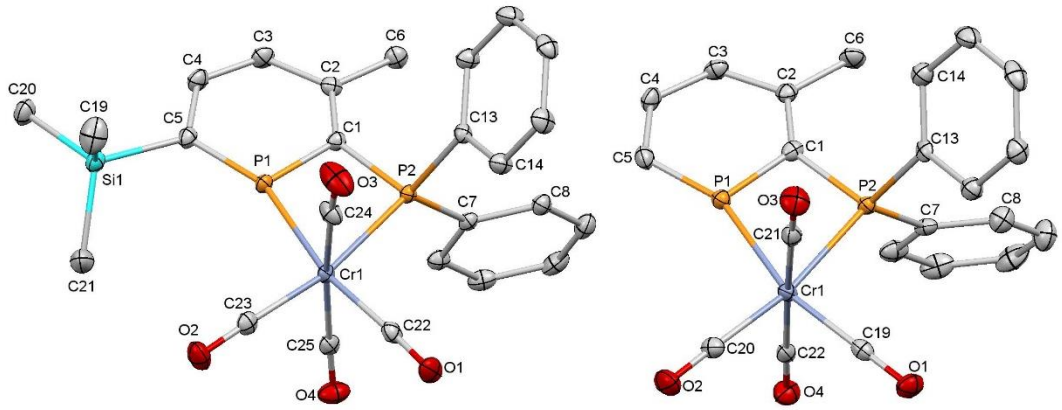

Upon desilylation, the A_1 CO stretch for the Cr and Mo carbonyl complexes (Table 1) is lowered by ca. 10 cm^{-1} indicating substantially poorer π-acceptance for the desilylated ligand **2**. This is in line with a previous computational investigation that predicted that the HOMO of phosphinine is higher in energy and the LUMO is lower in energy with *ortho*-silyl substituents.[41] However, a recent DFT comparison of 2-$SiMe_3PC_5H_4$ with PC_5H_5 suggested different behavior compared to phosphinophosphinines as it was calculated that the silyl group did not change the energy of the LUMO, but instead raised the energy of the phosphinine lone pair, such that it went from HOMO-2 to HOMO-1.[40] The values for *cis*-[$Mo(CO)_4L_2$] complexes allow comparisons between ligands to be made.[46] Ligand **1** (ν = 2026 cm^{-1}) was observed to be more π-accepting than dppm (ν = 2020 cm^{-1})[58] and $(PPh_3)_2$ (ν = 2022 cm^{-1}),[46] whereas ligand **2** (ν = 2017 cm^{-1}) is less π-accepting. A value of 2028 cm^{-1} for a related chelating pyridyl-phosphinine complex[49] is very similar to **1**. The relatively small differences compared to PPh_3 or dppm are consistent with

half of the ligand resembling PPh_3. The IR stretching data therefore suggests that these ligands would be suitable candidates in catalysis where small bite angle aryl phosphine donors are predominant,[16] such as ethylene oligomerization reactions.

Stability of 2-phosphinophosphinines

Complex **6** was found to be thermally unstable as shown by heating a benzene solution to 80°C which formed insoluble precipitate and several new soluble phosphorus-containing species that could not be characterised further. Evidence for one decomposition pathway was found upon slow decomposition of **6** at room temperature in the presence of water vapour from the air where **6** was found to convert to a dinuclear species (Scheme 3) amongst a number of other unidentified decomposition products. X-ray diffraction experiments of single crystals grown from the slow diffusion of hexane into a CH_2Cl_2 solution revealed the molecular structure of **8** (Figure 3) which demonstrated that two complexes had reacted together in manner that resembles 4 + 2 cycloaddition, followed by addition of H_2O that would be facile with the resultant isolated P=C bonds. Although no further analytical data could be obtained, the reaction casts light on another effect of removing $SiMe_3$ substitution from the phosphinine 6-position because $SiMe_3$ substitution would hinder the ability of the phosphinine to act as a diene in this manner. Additional, unwanted reactivity of a ligand contributes towards catalyst instability and represents a very important, but often overlooked, area of catalyst design, as well as highlighting a computationally challenging field – computational studies can be used to test mechanistic hypotheses, but the discovery of novel reactivity cannot normally be achieved.

Scheme 3. Dimerization of **6** and addition of H_2O to form dinuclear **8**.

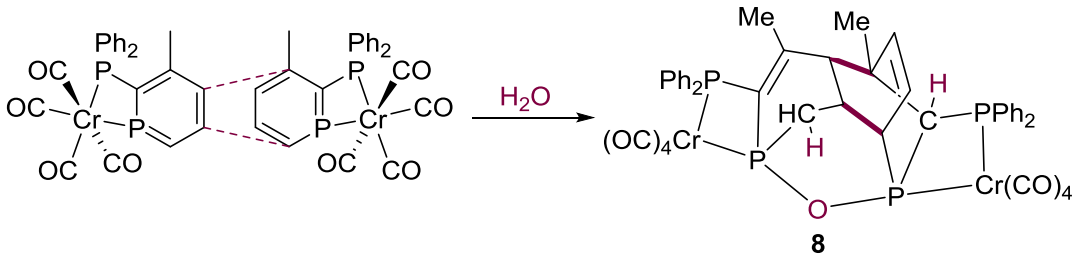

Figure 3. Thermal ellipsoid plot of the molecular structure of **8** (50% probability). The phenyl rings are displayed as capped sticks and without hydrogen atoms for clarity

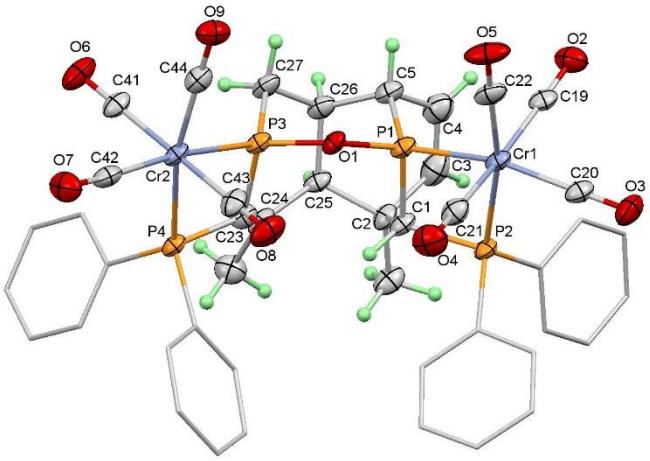

Reactions of phosphinines with lithium alkyls have been shown to give anionic phosphacyclohexadienyl anions.[59-62] These species can act as ligands either through the P lone pair, usually when another donor is present as a substituent on the phosphinine ring and the ligand can chelate,[35, 61, 63-67] or through the π-system.[61, 68-70] It has been reported that Et_2AlOEt reacts with 2,4,6-triphenylphosphinine and $[Ni(acac)_2]$ to generate a dinuclear complex with one Ni bound to the π-systems of two P-ethyl phosphacyclohexadienyl anions with the second Ni binding η^1 to the P atoms and an ethene ligand.[71] This reactivity with an aluminium alkyl

prompted us to explore the reaction of MAO with **1** and complex **3**, as a surrogate for the paramagnetic species formed in the catalytic reactions, in an analogous manner to dppm reactivity studies.[28] In reactions with 30 equivalents of MMAO-12, **1** and **3** showed no significant change in color, which would have been expected for the intensely colored phosphacyclohexadienyl anions,[37, 61-62] and retained the high frequency ^{31}P NMR spectroscopic resonances observed in the starting materials which are characteristic of aromatic phosphinines. Extended reaction still did not lead to reaction of the phosphinine centers indicating that phosphinophosphinine ligands are resistant to reaction with MAO.

Computational insight

The properties of ligands can be captured by a range of steric and electronic parameters,[72-73] and organometallic catalysis has a long tradition of relying on such data to guide catalyst optimisation.[44, 74] While such parameters can be determined experimentally, such an approach becomes particularly powerful when computational approaches can be used to evaluate novel ligand structures,[75] contextualising their likely properties before synthesis.[76-77] The ligand knowledge base (LKB) approach developed in Bristol and described in detail elsewhere,[78-81] captures the properties of ligands in different coordination environments from relatively straightforward optimisations of ground state structures using standard density functional theory (DFT) calculations.[79] A range of structural parameters, energies and steric properties are extracted from these calculations (Table S5) and have been used in regression models, but also processed with a statistical projection technique, Principal Component Analysis (PCA), to optimally represent ligand similarities as distances on a so-called map of chemical space.[72] As shown recently for monodentate ligands,[82] such maps, where proximity indicates ligands with

similar properties, can set unusual ligand designs, including phosphinines,[30-32, 35] into context and so suggest possible applications in catalysis.

Chart 2: Ligands discussed for LKB-PP (labels in bold correspond to those used elsewhere in this work).

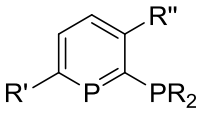

N1, **1**, R = Ph, R' = $SiMe_3$, R'' = Me
N2, **2**, R = Ph, R' = H, R'' = Me
N3, R = Ph, R' = $SiMe_3$, R'' = H
N4, R = Ph, R' = H, R'' = H
N5, R = Ph, R' = Si^iPr_3, R'' = Me
N6, R = Me, R' = $SiMe_3$, R'' = Me
N7, R = ^{n}Bu, R' = $SiMe_3$, R'' = Me
N8, R = ^{i}Pr, R' = $SiMe_3$, R'' = Me
N9, R = ^{t}Bu, R' = $SiMe_3$, R'' = Me
N10, R = Me, R' = H, R'' = Me
N11, R = ^{n}Bu, R' = H, R'' = Me
N12, R = ^{i}Pr, R' = H, R'' = Me
N13, R = ^{t}Bu, R' = H, R'' = Me

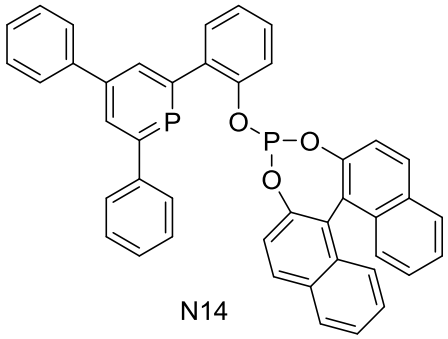

N14

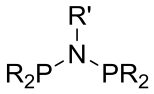

16, R = Ph, R' = H
21, R = Ph, R' = Me
22, R = *o*-tolyl, R' = Me
24, **A**, R = *o*-OMe-C_6H_4, R' = Me
31, **B**, R = Ph, R' = ^{i}Pr
35, R, R' = Ph

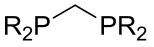

3, R = ^{t}Bu
5, **C**, R = Ph
7, R = *o*-tolyl
8, R = *o*-OMe-C_6H_4

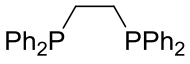

52, **F**

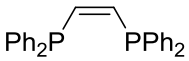

71, **G**

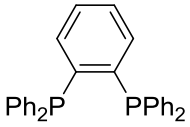

77, **H**

Having established the bidentate nature of ligands **1** and **2**, we were interested in how they compared to other small bite angle ligands, including some of those shown in Chart 1 – if their

properties are very similar to known bidentate ligands, they will appear in close proximity to these on a PCA map. In addition, we used this approach to explore synthetically accessible structural variations computationally, with a view to quantifying their impacts on ligand properties and so selecting the most promising targets. Chart 2 shows the ligands added to the relevant LKB (LKB-PP),[79] alongside the labelling of relevant ligands published previously; note that the labelling of ligands is in line with previously published LKB-PP data and so specific to this section only. Tables of all ligands (Table S4) and parameters (Table S5), as well as the data for new ligands (Table S6) and further details of the principal component analysis (Tables S7-8) can be found in the electronic supporting information. Attaching chemical meaning to principal components is difficult, both because this approach is not statistically robust, i.e. composition changes when the ligand set is changed, and because ligand property parameters extracted from calculations on representative molecular systems are rarely due to a single effect. In most settings, both steric and electronic effects combine to give rise to an observable. Here, in the interest of brevity, discussion will focus on the maps resulting from PCA analysis. Figure 4 shows the updated LKB-PP map of ligand space with ligands N1-N14 added.

Figure 4. Ligand map generated by principal component analysis of 28 ligand parameters capturing the structures and energies of 324 P,P-donor ligands through DFT-calculated parameters, collected in LKB-PP. The principal components are linear combinations of the original parameters derived to capture most of the variation in fewer uncorrelated parameters (58% in this case). Each symbol corresponds to a ligand, and shape and colour are determined by substituents as shown in the legend. See Figure S58 for more detailed labels.

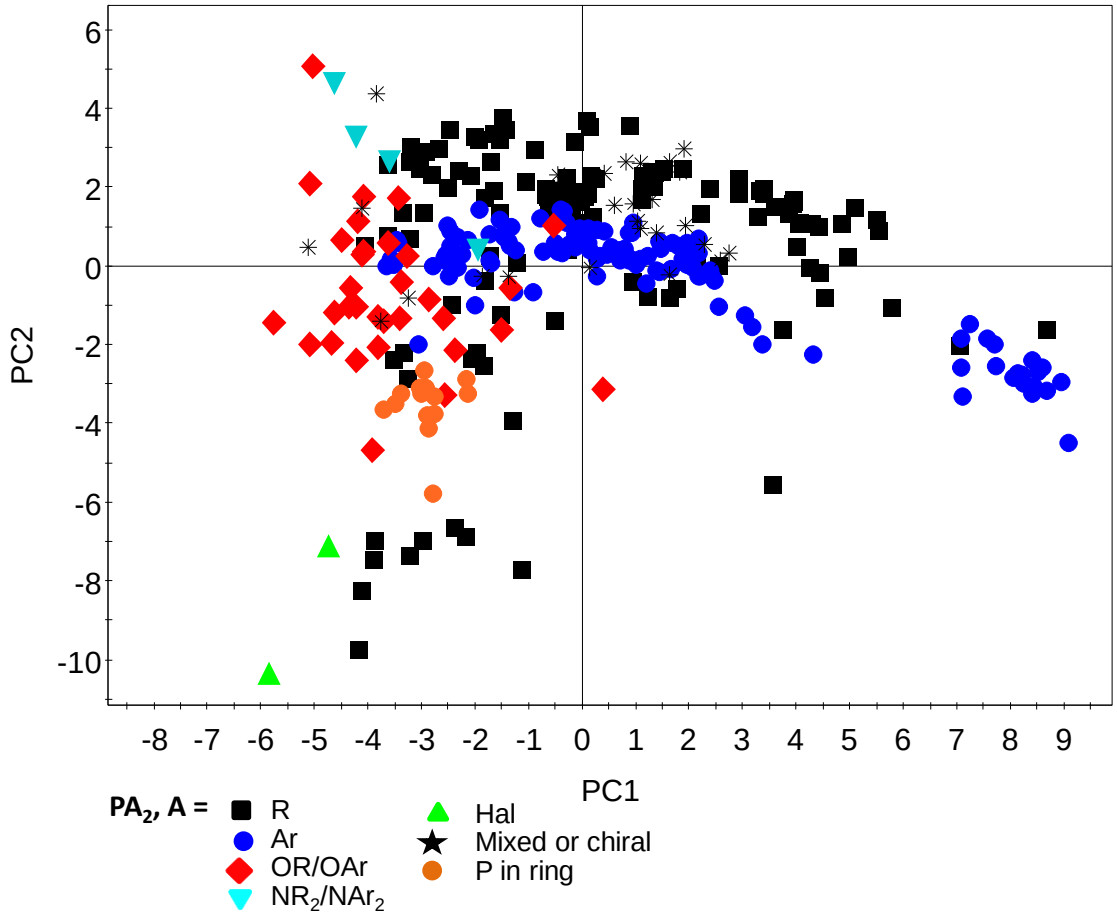

The ligand map shown in Figure 4 places the new ligands (orange dots) towards the edge of ligand space, but generally these are closer, and so more similar, to other ligand architectures than halide substituted ligands. Figure 5 shows the area of the LKB-PP map closest to the phosphinine ligands, including labels for all ligands shown in Chart 2.

Figure 5. Ligand map focussing on ligands N1-N14. See Chart 2 for ligand labels and Figure S60 for a more comprehensively labelled version. Red boxes highlight the exceptional PNP ligands **A** (24) and **B** (31) for ethylene oligomerisation and the phosphinophosphinines **1** and **2**.

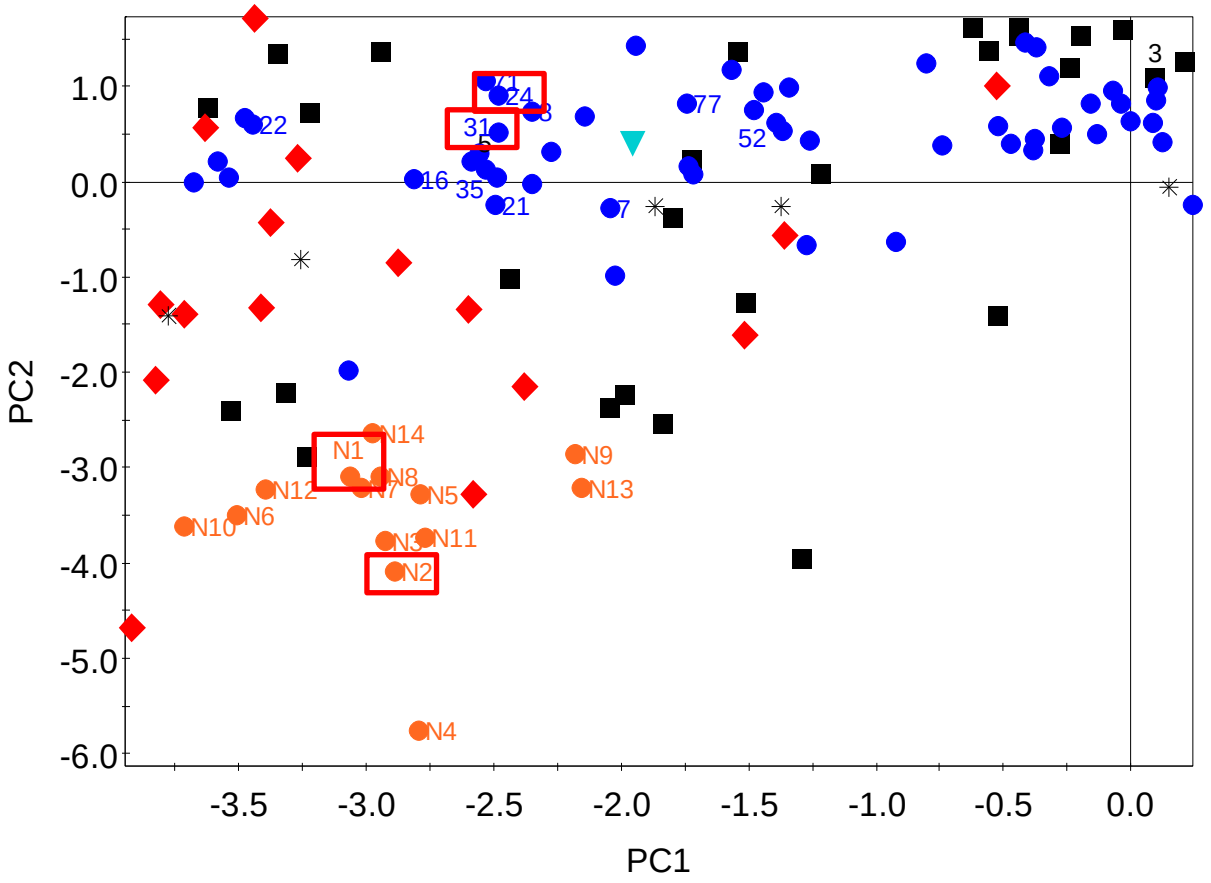

Considering the 2-phosphinophosphinine ligands, the removal of the $SiMe_3$ substituent alters the ligand properties, with N2 and N4 lying slightly further away from the other ligands. Where the phosphorus donor is more electron rich (N6-N9 vs. N10-N13), these differences appear less pronounced, suggesting that such ligand modifications are a fine balance of steric and electronic effects, and that it may be possible to fine-tune catalytic activity through changing these substituents. This map also suggests that although similar in the first principal component, these new ligands are likely to have somewhat different properties compared to other small bite angle PNP and PCP ligands, as identified by their differences in the second principal component.

Figure 6: Plot of PC1 and PC3, focussing on ligands N1-N14. See Chart 2 for ligand structures and Figure S61 for more comprehensive labels in this area. Red boxes highlight the exceptional PNP ligands **A** (24) and **B** (31) for ethylene oligomerisation and the phosphinophosphinines **1** and **2**.

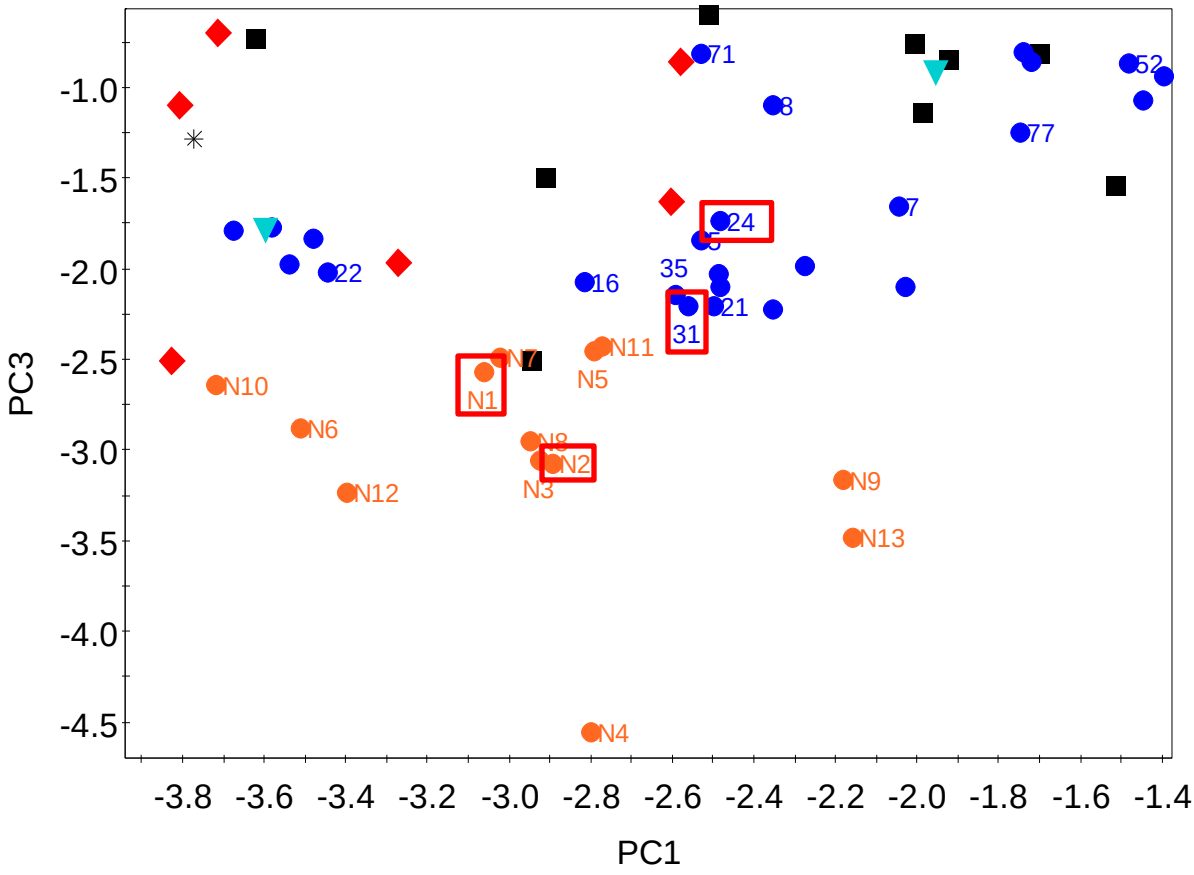

Figures 4 and 5 focus on PC1 and PC2, which capture 58% of the variation in this database, but it is worth noting that 28 parameters will give rise to 28 principal components and in the case of bidentate ligands, consideration of PC3 will capture 66% of the variation, with PC4 taking this to 73%. Without relating this to extensive experimental datasets, it is difficult to determine which PCs are most important in terms of the catalysis of interest, and in the present case it will be

sensible to consider PC3 as well (Figure S59, Figure 6). Interestingly, a plot of PC1 vs. PC3 places the small bite-angle ligands quite close together (Figure 6), regardless of backbone, further emphasising that additional principal components may need to be considered in the analysis of such bidentate ligands. While 2-phosphinophosphinine ligands remain slightly separate from other ligand architectures, changing the Si substituents (N5) or making the phosphine donor more electron rich without increasing steric hindrance near to the coordinating site (^{n}Bu, N11) appears to move ligands towards the privileged PNP ligands (including 31).

This analysis of ligand properties highlights that 2-phosphinophosphinine ligand properties can be tuned by altering substituents, which will support the selection of a more extensive and varied set for future synthesis and testing in catalysis. Synthetically accessible changes can be evaluated computationally, guiding synthesis to the most promising modifications.

Ethylene oligomerization catalysis

Ligands **1** and **2** were screened for ethylene oligomerisation catalysis under typical conditions (Scheme 4, Table 2). The results quoted for ligand **1** are an average of four reactions, and for ligand **2** an average of two reactions. Data for the individual repeats are summarised in the ESI, along with representative GC traces and details of the catalysis procedure and equipment used. In order to provide benchmarks for comparison, a reaction was also performed under the same conditions with no ancillary ligand present, and another reaction using the standard PNP ligand Ph_2P-N(^{i}Pr)-PPh_2 (ligand **B** in Chart 1).

As can be seen from Table 2, entry 1, when no ancillary ligand is used, $Cr(acac)_3$ and MMAO-3A activator under these conditions give almost exclusively polymer (98.0 wt%) as the reaction

product, whilst the trace liquid fraction is a Schulz-Flory distribution overlaid with some selective trimerisation of ethylene to 1-hexene (see Figure 7a). This highlights the importance of blank reactions, as $Cr(acac)_3$ is capable of a small degree of selective trimerisation with no ancillary ligand present. Catalysis using ligands **1** and **2** (entries 3 and 6) serves to slightly lower the activity, but the selectivity is vastly improved, with the polymer fraction reduced to 15.1 and 36.5 wt% on average, respectively. Furthermore, the selectivity is strongly perturbed towards selective trimerisation and tetramerisation (see Figure 7c and 7d), although there is a trace of Schulz-Flory oligomerisation still present. However, further examination reveals that the formation of cyclic products is extremely high, with cyclic species being observed throughout the product spectrum (see GC traces in ESI) and accounting for much of the Schulz-Flory behaviour observed. This is an interesting observation as the formation of cyclic products is believed to stem from the key chromacycloheptane intermediate (see Scheme 1, introduction) from which 1-hexene may be liberated or further growth to larger metallacycles (producing 1-octene in due course) may occur.[11] Isomerization of the chromacycloheptane intermediate forms a methylcyclopentane ligand that can then insert ethylene which ultimately forms longer chain alkyl- and alkenyl-cyclopentanes via two different pathways (Scheme 1).[12-15] Although small amounts are produced with ligand **B**,[11] a high percentage of cyclopentane products has been recently observed for several heteroditopic P,S and homoditopic S,S ligands in Cr catalysed ethylene oligomerization.[12] 1-PPh_2-2-SMe-C_6H_4 was the most active ligand and also generated a large amount of cyclic products because it was observed that increasing steric bulk tended to supress formation of C10+ oligomers.[12] Comparing the ratios of alkenylcyclopentanes to alkylcyclopentanes showed ratios close to 1 for PNP ligand **B** over many different chain lengths[14] (similar to **1**), whereas 1-PPh_2-2-SMe-C_6H_4 gave ratios that varied from 4.2 for C6 to

ca. 2 for C8+, which only converged towards 1 with much longer chain lengths of alkenyl- and alkyl-cyclopentanes.[12] Interestingly, the pendant ether-donor PNP ligands $Ph_2PN(R)PPh_2$, where R = *o*-$OSiMe_3C_6H_4$, $C_2H_4OSiMe_3$ and C_2H_4OBn, have also shown high levels of alkyl and alkenyl-cyclopentanes.[15] These results indicate that the nature of the ligand can affect both the barrier heights producing either saturated or unsaturated cyclic products, as well as the fraction of these products.

Comparison with the benchmark Ph_2P-N(^{i}Pr)-PPh_2 ligand (entry 2) reveals that ligands **1** and **2** are not competitive with the industry standard system, but rather provide a different selection of products. In comparing the effect of silyl substitution, ligand **2** gave a better selectivity to 1-hexene and 1-octene within the liquid fraction, but the activity was lower compared to ligand **1**, and the polymer formation level was doubled. Thus, simple correlation of ligand donor properties and steric hindrance to catalytic performance is insufficient in this case, highlighting that ligand design is still a complex challenge, likely requiring more extensive mechanistic study.

Scheme 4. Catalytic ethylene oligomerization

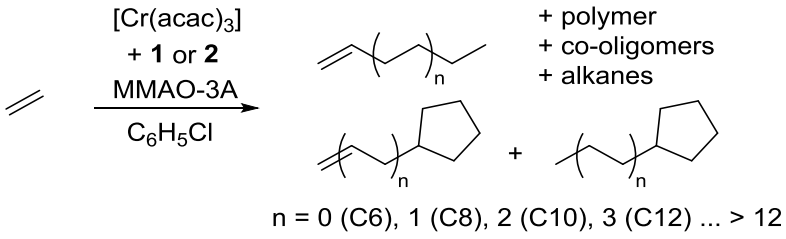

In order to explore the scope for improvement of performance with ligand **1**, a reaction was performed using a different activation method. Rather than activation under dilute conditions *in situ* in the reactor, a concentrated pre-activation in a Schlenk tube was employed (Table 2, entry 4). Whilst the activity and selectivity within the liquid fraction were essentially unchanged, the

polymer formation level doubled. Another alternative procedure examined was to halve the chromium concentration (Table 2, entry 5); this led to a doubling of the activity, and a slight increase in polymer formation, whilst the selectivity within the liquid fraction remained unchanged.

Figure 7. Graphs of the liquid fraction product slate obtained for catalysis from Table 2: a) entry 1, no ligand; b) entry 2, PNP ligand; c) entry 3, ligand **1**; d) entry 6, ligand **2**. The green bars represent 1-olefin, blue bars alkyl- and alkenylcyclopentanes, and the white bars other structural isomers and alkanes.

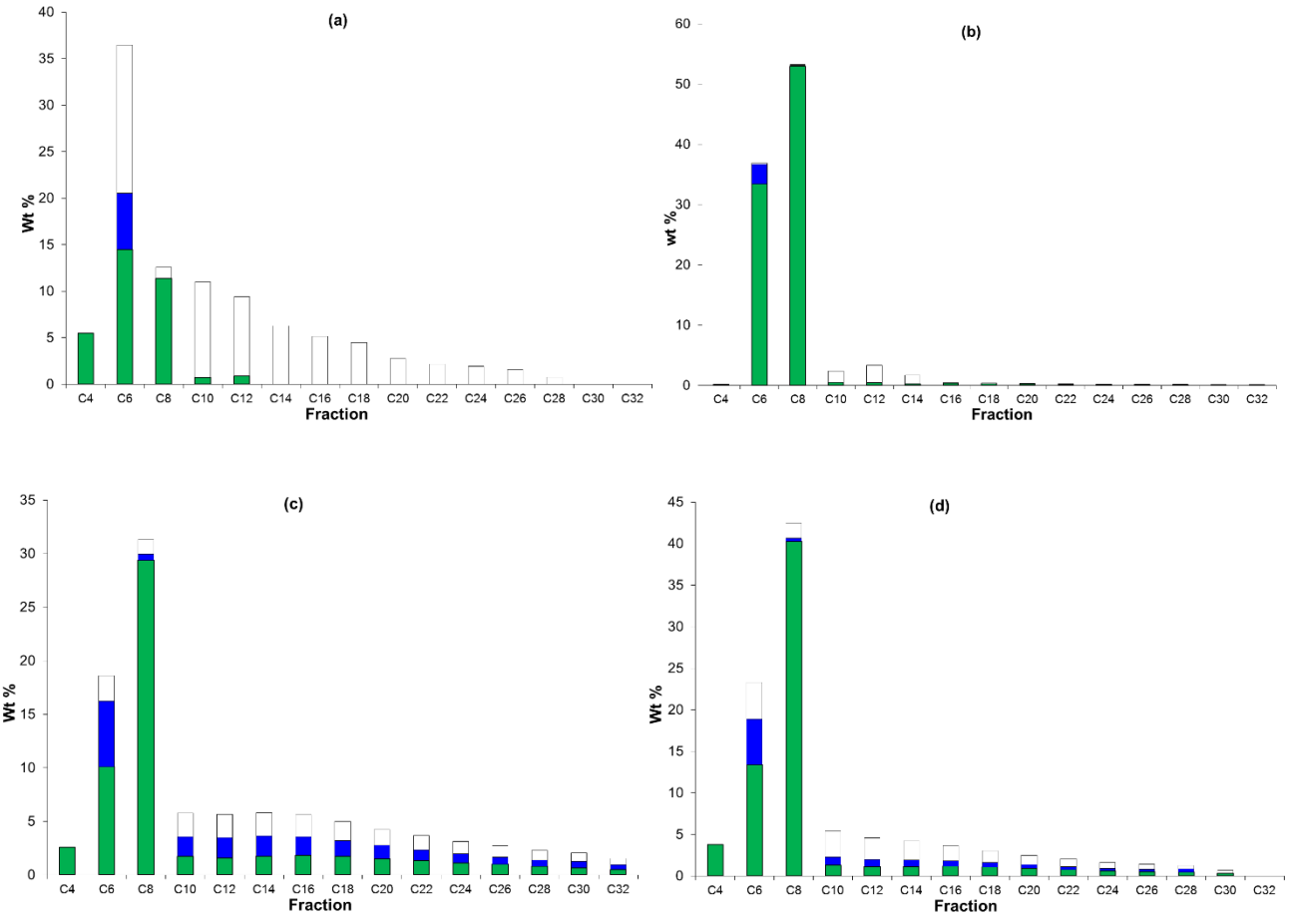

Table 2. Selective ethylene oligomerisation catalysis data. General reaction conditions: $Cr(acac)_3$ 5 µmol, Ligand 1.2 eq, MMAO-3A 1000 eq, PhCl 65 mL, 40 barg ethylene (41 bara), 60 °C, 250 mL reactor. [a] wt% of liquid fraction. [b] wt% of total product slate. [c] $Cr(acac)_3$ 1.25 µmol. [d] concentrated pre-activation in a Schlenk. [e] $Cr(acac)_3$ 2.5 µmol.

Entry	**Ligand**	**Time {min}**	**Productivity {g/gCr}**	**Activity {g/gCr/h}**	**1-C_8 + 1-C_6 {wt%}** [a]	**1-C_8 / 1-C_6**	**C_4 {wt%}** [a]	**C_6 (1-C_6) {wt%}** [a]	**Cyc-C_6 {wt%}** [a] **(% of C_6)**	**C_8 (1-C_8) {wt%}** [a]	**C_{10-14} {wt%}** [a]	**C_{15+} {wt%}** [a]	**PE {wt%}** [b]
1	none	8.0	23,654	176,671	25.9	0.78	5.5	36.5 (39.8)	6.0 (16.5)	12.6 (90.6)	26.7	18.8	98.0
2 [c]	Ph_2P-N(^{i}Pr)-PPh_2	16.2	624,014	2,318,320	86.4	1.58	0.2	36.9 (90.6)	3.3 (8.9)	53.3 (99.4)	7.4	2.3	0.98
3	**(1)**	30.0	15,604	31,200	37.1	2.83	2.3	18.4 (52.6)	6.5 (35.5)	29.5 (93.0)	17.5	32.3	15.1
4 [d]	**(1)**	30.0	14,534	29,068	40.0	2.74	2.6	19.3 (55.4)	6.2 (32.2)	31.2 (93.9)	16.6	30.3	28.3
5 [e]	**(1)**	30.0	27,693	55,387	34.2	2.32	1.8	18.8 (54.8)	6.7 (35.7)	25.9 (92.3)	18.2	35.4	19.0
6	**(2)**	30.0	6,061	12,122	53.8	2.84	3.8	24.0 (58.6)	5.5 (22.9)	42.0 (94.7)	14.2	16.2	36.5

Conclusions

This work has shown that 2-phosphinophosphinines are a useful class of ligands for homogeneous catalysis with extremely small bite-angles and tuneable properties. Ligands with trimethylsilyl substitution at the 6-position, which is readily achieved synthetically, also allows access to a hydrogen atom in the 6-position by simple reaction with HCl, dramatically changing the steric profile and π-accepting properties of the phosphinine. Computational mapping of ligand properties, using Bristol's Ligand Knowledge Base approach (LKB-PP) has identified that 2-phosphinophosphinies inhabit an area of ligand space close to aryl-substituted PNP ligands suggesting their application in known catalytic reactions, but with distinct ligand properties as identified by principal component analysis. When used in the catalytic oligomerization of ethylene, 1-hexene and 1-octene production were identified, as anticipated by the computational mapping of ligand space, but in addition we have identified that these ligands promote a third pathway from the chromacycloheptane intermediate, producing alkyl- and alkenylcyclopentanes in significant quantities. The computational analysis also highlights that the properties of these ligands are responsive to changes in their substitution pattern, and that such fine-tuning can be captured by and illustrated on ligand property maps, supporting the rational selection of ligands for synthesis and testing in catalysis. There is therefore the potential in the future to use ligand mapping and ligand design to target new products from the industrially-important oligomerization of ethylene.

Experimental

All experiments were performed under dry, oxygen free N_2 using standard Schlenk-line and glovebox techniques. Dry and degassed solvents were collected from an MBraun SPS-800

solvent purification system (toluene, THF, CH_2Cl_2) or distilled from an appropriate drying agent under N_2: 40 -60 petroleum spirit (Na wire), Et_2O (Na/benzophenone). Benzene-d6 was dried over molten potassium and $CDCl_3$ was dried over CaH_2 and vacuum-distilled prior to use. Air sensitive samples for NMR spectroscopy were prepared in NMR tubes equipped with a Youngs tap. NMR spectra were recorded on Bruker AVIII400 (400 MHz), AVI400 (400 MHz) or AVIII300 (300 MHz) spectrometers at 25 °C unless otherwise noted. ^{1}H and ^{13}C NMR spectra were referenced to internal residual protio-solvent resonances, ^{11}B, ^{29}Si and ^{31}P NMR spectra were referenced to external samples of $BF_3.OEt_2$, $SiMe_4$ and 85% H_3PO_4 in H_2O respectively as 0 ppm. Mass spectrometry analysis was performed at the EPSRC UK National Mass Spectrometry Facility at Swansea University using an Atmospheric Solids Analysis Probe interfaced to a Waters Xevo G2-S (**3**, **5**, **6**, **7**),using EI on a MAT95 instrument (**2**), or at the University of Edinburgh using EI on a ThermoElectron MAT 900 (**4**). FTIR was performed on a Thermo Scientific Nicolet iS5/iD5 ATR spectrometer. Elemental analyses were conducted by Dr Brian Hutton using an Exeter CE-440 elemental analyser at Heriot-Watt University or by Mr Stephen Boyer at London Metropolitan University. The supporting information gives details for the catalytic reactions. All calculations were performed as previously described,[78] see the supporting information for further details. The following starting materials were synthesised according to literature procedures: **1.BH$_3$** and **1**,[37] [M(CO)$_4$(NBD)] M = Cr and Mo,[83] and [W(CO)$_4$(COD)].[84]

Synthesis of 2-(diphenylphosphine-borane)-3-methylphosphinine (2.BH$_3$)

1.BH$_3$[37] (1.01 g, 2.65 mmol, 1 equiv.) was dissolved in dry CH_2Cl_2 (15 cm^3) and a 1 M solution of HCl in Et_2O (2.65 cm^3, 2.65 mmol) was added. The reaction was stirred at room temperature for 24 h, then the volatiles were removed under reduced pressure yielding a pale

cream solid. The product was recrystallized from toluene at -25°C yielding **2.BH$_3$** as a colourless crystalline solid (432 mg, 1.40 mmol, 53 %).

^{1}H NMR (400 MHz, $CDCl_3$): δ = 8.59 (m, 1H, 6-*H*), 7.85 (m, 1H, 5-*H*), 7.73 (m, 4H, *o*-P*Ph$_2$*), 7.59-7.44 (m, 7H, *m*- and *p*-P*Ph$_2$* and 4-*H*), 2.55 (s, 3H, 3-C*H$_3$*), 2.12-0.87 (bm, 3H, B*H$_3$*); ^{13}C NMR (100 MHz, $CDCl_3$): δ = 156.6 (dd, phosphinine C), 151.4 (dd, phosphinine CH), 150.4 (m, 2 overlapping phosphinine CH), 135.3-135.1 (m, PPh_2), 133.8-133.5 (m, PPh_2), 131.4 (d, PPh_2), 129.8-129.1 (m, phosphinine CH), 128.8 (d, PPh_2), 26.1 (d, C(*C*H$_3$), $^3J_{C\text{-}P}$ = 7.4 Hz); ^{31}P NMR (162 MHz, $CDCl_3$): δ = 229.7 (d, $^2J_{P\text{-}P}$ = 79.8 Hz, 1-*P*), 23.0 (bs, 2-*P*); ^{11}B NMR (128 MHz, $CDCl_3$): δ = -36.0 (bs, *B*H$_3$); Anal. Calcd. for $C_{18}H_{19}BP_2$: C 70.17, H 6.22; Found: C 70.11, H 6.14.

Synthesis of 2-(diphenylphosphino)-3-methylphosphinine (2)

Method A: 1 M HCl in Et_2O (1.4 cm^3, 1.4 mmol, 1 equiv.) was added to a solution of **1** (512 mg, 1.40 mmol, 1 equiv.) in CH_2Cl_2 (10 cm^3) and the reaction was stirred for 24 h. All volatiles were removed under reduced pressure and the resulting solid was dried under high vacuum. The product was then recrystallized from 40-60 petrol at -25°C producing **2** as colourless microcrystalline material (319 mg, 1.08 mmol, 77%).

Method B: **2.BH$_3$** (174 mg, 0.565 mmol) was deprotected by stirring with 0.5 equivalents of DABCO (32 mg, 0.282 mmol) in toluene (10 cm^3) for 2 days. The mixture was filtered and then all volatiles were removed under reduced pressure. The product was then recrystallised from petroleum ether yielding **2** as a colourless solid (144 mg, 0.489 mmol, 87%). ^{1}H NMR (300 MHz, 25 °C, C_6D_6): δ = 8.37 (dd, 1H, 6-*H*, $^2J_{H\text{-}P1}$ = 40.7 Hz, $^3J_{H\text{-}H}$ = 9.9 Hz), 7.46-7.40 (m, 4H, *o*-PPh_2), 7.30 (m, 1H, 5-*H*), 7.06-7.04 (m, 6H, *m*- and *p*-PPh_2), 6.94-6.89 (m, 1H, 4-*H*) 2.42 (s, 3H, 3-C*H$_3$*); ^{31}P NMR (121 MHz, 25 °C, C_6D_6): δ = 224.9 (d, 1-*P*, $^2J_{P\text{-}P}$ = 31.2 Hz), -7.6 (d, 2-*P*,

$^2J_{P\text{-}P}$ = 31.2 Hz); HRMS (EI/MS) m/z Calc. for $C_{18}H_{16}P_2$ 294.0722 $[M]^+$; Found 294.0715; Anal. Calcd. for $C_{18}H_{16}P_2$: C 73.45, H 5.48; Found: C 73.39, H 5.45. Data match literature values.[42]

Synthesis of [Cr(1)(CO)$_4$] (3)

[Cr(NBD)(CO)$_4$] (72 mg, 0.273 mmol) and one equivalent of **1** (101 mg, 0.273 mmol) were dissolved in toluene (20 cm^3) and stirred at 60°C for 24 h, during which time the solution turned from yellow-orange to red-orange. Volatile solvent and NBD were evaporated under reduced pressure forming an orange oil, which was washed with petroleum ether forming a solid. This solid was dissolved in toluene, and orange crystals formed when the solution was cooled to-25°C for 24 h. These were isolated by filtration and dried under vacuum (109 mg, 0.204 mmol, 75%). ^{1}H NMR (400 MHz, $CDCl_3$): δ = 7.88 (ddd, J = 23.2, 8.5, 1.5 Hz, 1H, 5-*H*), 7.60 (m, 4H, PPh_2), 7.47 (m, 6H, PPh_2), 7.00 (app. dt, J = 8.8, 3 Hz, 1H, 4-*H*), 1.94 (s, 3H, 3-C*H*$_3$), 0.42 (s, 9H, $SiMe_3$); ^{13}C NMR (100.6 MHz, $CDCl_3$): δ = 229.3 (dd, J = 13.6, 1.6 Hz, CO), 227.5 (dd, J ≈ 11, 3 Hz, CO), 221. 9 (dd, J = 17.8, 11.9 Hz, CO), 166.5 (dd, J = 13.4, 4.5 Hz, phosphinine C), 164.0 (dd, J = 52.0, 20.8 Hz, phosphinine C), 146.1 (app. d, J ≈ 11, 5 Hz, phosphinine C), 144.6 (dd, J = 14.9, 3.0 Hz, phosphinine CH), 133.1 (dd, J = 28.2, 10.4 Hz, *ipso*-Ph C), 131.6 (d, J = 11. 9 Hz, *o*-Ph CH), 130.3 (s, *p*-Ph CH), 128.9 (d, J = 8.9 Hz, 5.94 Hz, *m*-Ph CH), 127.0 (dd, J = 34.2, 6.0 Hz, phosphinine CH), 21.7 (app. t, J = 5.9 Hz, CH_3), -0.3 (d, J = 3.0 Hz, $SiMe_3$); ^{31}P NMR (162 MHz, $CDCl_3$): δ = 273.6 (d, $^2J_{PP}$ = 38.2 Hz, 1-*P*), 40.5 (d, $^2J_{PP}$ = 38.2 Hz, 2-*P*); ^{29}Si NMR (79.5 MHz, $CDCl_3$): δ = -1.1 (dd, $^2J_{SiP}$ = 21.6, $^4J_{SiP}$ = 2.6 Hz, $SiMe_3$); HRMS (ASAP/QTof) m/z Calc. for $C_{25}H_{25}CrO_4P_2Si$: 531.0403 $[M+H]^+$; Found 531.0404; FTIR (ATR): ν(cm^{-1}) 1895 (CO), 1906 (CO), 2013 (CO); Anal. Calc. for $C_{25}H_{24}O_4P_2SiCr$: C 56.60, H 4.56; Found: C 56.50, H 4.63.

Synthesis of [Mo(1)(CO)$_4$] (4)

[Mo(NBD)(CO)$_4$] (85 mg, 0.280 mmol) and one equivalent of **1** (103 mg, 0.280 mmol) were reacted as above at 20°C for 2 h yielding the product as pale yellow crystals (48 mg, 0.09 mmol, 30%). ^{1}H NMR (400 MHz, $CDCl_3$): δ 7.93 (ddd, J = 22.6, 8.5, 2.1 Hz, 1H, 5-*H*), 7.58 (m, 4H. PPh_2), 7.47 (m, 6H, PPh_2), 7.06 (m, 1H, 4-*H*), 1.93 (s, 3H, 3-C*H*$_3$), 0.44 (s, 9H, $SiMe_3$). ^{13}C NMR (100 MHz, $CDCl_3$): δ = 219.1 (dd, J = 31.2, 8.9 Hz, CO), 217.8 (dd, J = 26.8, 8.9 Hz, CO), 210.3 (dd, J ≈ 11, 8 Hz, CO), 168.5 (d, J = 14.9 Hz, phosphinine C), 161.1 (dd, J = 52.0, 19.3 Hz, phosphinine C), 148.0 (dd, J = 11.9, 6.0 Hz, phosphinine C), 143.8 (d, J = 17.8 Hz, phosphinine CH), 133.0 (dd, J = 28.2, 10.4 Hz, *ipso*-Ph C), 131.7 (d, J = 11.9 Hz, *o*-Ph CH), 130.2 (s, *p*-Ph CH), 128.9 (d, J = 8.9 Hz, *m*-Ph CH), 127.7 (dd, J = 34.2, 4.5 Hz, phosphinine CH), 21.9 (app. t, J = 6.0 Hz, CH_3), -0.3 (d, J = 3.0 Hz, $SiMe_3$). ^{31}P NMR (162 MHz, $CDCl_3$): δ 244.8 (d, $^2J_{PP}$ = 72.8 Hz, 1-*P*), 18.9 (d, $^2J_{PP}$ = 72.8 Hz, 2-*P*); ^{29}Si NMR (80 MHz, $CDCl_3$): δ -0.8 (dd, $^2J_{SiP}$ = 22.1, $^4J_{SiP}$ =2.7 Hz, $SiMe_3$); MS (EI/MS) m/z: 576.0 ([M]$^+$, 6.3%); FTIR (ATR): ν(cm^{-1}) 1888 (CO), 1926 (CO), 2026 (CO); Anal. Calc. for $C_{25}H_{24}O_4P_2SiMo$: C 52.27, H 4.21; Found: C 52.14, H 4.36.

Synthesis of [W(1)(CO)$_4$] (5)

[W(COD)(CO)$_4$] (110 mg, 0.273 mmol) and one equivalent of **1** (101 mg, 0.273 mmol) were reacted as above at 75°C for 4 d yielding the product as red crystals (125 mg, 0.188 mmol, 69%). ^{1}H NMR (300 MHz, $CDCl_3$): δ = 7.95 (ddd, J = 24.6, 8.4, 2.6 Hz, 1H, 5-*H*), 7.58 (m, 4H, PPh_2), 7.47 (m, 6H, PPh_2), 7.06 (m, 1H, 4-*H*), 1.93 (s, 3H, 3-C*H*$_3$), 0.44 (s, 9H, $SiMe_3$); ^{13}C NMR (75 MHz, $CDCl_3$): δ = 210.0 (dd, J = 31.0, 6.6 Hz, CO), 209.0 (dd, J = 24.3, 7.7 Hz, CO), 203.7 (dd, J = 10.0, 6.6 Hz, CO), 172.0 (d, J = 21.0 Hz, phosphinine C), 155.8 (dd, J = 44.2, 21.0 Hz, phosphinine C), 149.7 (dd, J = 12.2, 5.5 Hz, phosphinine C), 143.8 (dd, J = 17.7 Hz, 3 Hz phosphinine CH), 131.9 (dd, J = 34.3, 11.1 Hz, *ipso*-Ph C), 131.8 (d, J = 13.3 Hz, *o*-Ph CH),

130.5 (s, *p*-Ph CH), 128.9 (d, J = 10.0 Hz, *m*-Ph CH), 126.5 (dd, J = 35.4, 5.5 Hz, phosphinine CH), 21.7 (app. t, J = 6.6 Hz, *C*H_3), -0.4 (d, J = 3.0 Hz, $SiMe_3$). ^{31}P NMR (121 MHz, $CDCl_3$,): δ 209.6 (d, $^2J_{PP}$ = 78.0 Hz. ^{183}W satellites: dd, $^1J_{WP} \approx 212$, $^2J_{PP}$ 78 Hz, 1-*P*), -0.1 (d, J = 78.0 Hz, ^{183}W satellites: dd, $^1J_{WP}$ = 200.3, $^2J_{PP}$ = 75.4 Hz, 2-*P*); ^{29}Si NMR (79.5 MHz, $CDCl_3$,): δ -0.7 (dd, $^2J_{SiP}$ = 20.9, $^4J_{SiP}$ =2.3 Hz, $SiMe_3$); HRMS (ASAP/QTof) m/z Calc. for $C_{25}H_{25}O_4P_2SiW$: 663.0509 $[M+H]^+$; Found 663.0508; FTIR (ATR): ν(cm^{-1}) 1883(CO), 1914 (CO), 2021 (CO); Anal. Calc. for $C_{25}H_{24}O_4P_2SiW$: C 45.34, H 3.65; Found: C 45.49, H 3.55.

Synthesis of [Cr(2)(CO)$_4$] (6)

[Cr(NBD)(CO)$_4$] (109 mg, 0.427 mmol) and one equivalent of **2** (126 mg, 0.427 mmol) were reacted as above at 65°C for 24 h yielding the product as red crystals (62 mg, 0.135 mmol, 32%). ^{1}H NMR (400 MHz, C_6D_6): δ = 7.71-7.61 (m, 1H, 6-*H*), 7.55-7.51 (m, 4H, *o*-PPh_2), 7.13-6.99 (m, 7H, 5-*H* & *m*,*p*-PPh_2), 6.37 (bs, 1H, 4-*H*), 1.52 (s, 3H, 3-C*H*$_3$); ^{13}C NMR (100 MHz, C_6D_6,): δ = 230.3 (d, J = 13.6 Hz, CO), 228.4 (dd, J = 11.2, 3.2 Hz, CO), 223.0 (dd, J = 17.6, 11.2 Hz, CO), 166.9 (dd, J = 15.2, 1.6 Hz, phosphinine C) 149.6 (dd, J = 28.0, 20.0 Hz, phosphinine CH), 146.9 (dd, J = 12.8, 7.2 Hz, phosphinine C), 140.6 (dd, J = 16.0, 3.2 Hz, phosphinine CH), 133.5 (dd, J = 28.8, 10.4 Hz, *ipso*-Ph C), 132.1 (d, J = 12.0 Hz, PPh_2), 130.8 (d, J = 2.4 Hz, PPh_2), 129.5 (d, J = 9.6 Hz, PPh_2), 128.6-128.2 (m, phosphinine CH and C_6D_6 overlapping), 21.9 (t, J = 7.2 Hz *C*H_3); ^{31}P NMR (162 MHz, C_6D_6): δ = 250.3 (d, $^2J_{PP}$ = 33.8 Hz, 1-*P*), 41.8 (d, $^2J_{PP}$ = 33.8 Hz, 2-*P*); HRMS (ASAP/QTof) m/z Calc. for $C_{22}H_{17}CrO_4P_2$: 459.0007 $[M+H]^+$; Found 459.0001; FTIR (ATR): ν(cm^{-1}) 1864 (CO), 1898 (CO), 2003 (CO); Anal. Calc. for $C_{22}H_{16}CrO_4P_2$: C 57.66, H 3.52; Found: C 58.08, H 3.44.

Synthesis of [Mo(2)(CO)$_4$] (7)

[Mo(NBD)(CO)$_4$] (20 mg, 0.068 mmol) and one equivalent of **2** (20 mg, 0.068 mmol) were dissolved in toluene (2 cm^3) and stirred at 20°C for 2 h, during which time a yellow precipitate was observed. All volatiles were removed under reduced pressure and the resulting solid was dried under high vacuum, yielding the product as an analytically pure pale yellow microcrystalline powder (20 mg, 0.041 mmol, 60%). ^{1}H NMR (400 MHz, C_6D_6): δ = 7.70-7.60 (m, 1H, 6-*H*), 7.49 (bs, 4H, *o*-PPh_2), 7.09-6.97 (m, 7H, 5-*H* & *m*,*p*-PPh_2), 6.37 (bs, 1H, 4-*H*), 1.52 (s, 3H, 3-C*H*$_3$); ^{13}C NMR (100 MHz, C_6D_6): δ = 218.8 (dd, J = 32.0, 9.6 Hz, CO), 217.5 (dd, J = 26.4, 8.8 Hz, CO), 210.3 (dd, J ≈ 11, 8 Hz, CO), 168.4 (dd, J = 16.8, 1.6 Hz, phosphinine C) 148.0 (dd, J = 12.0, 5.6 Hz, phosphinine CH), 146.4 (dd, J = 25.6, 19.2 Hz, phosphinine C), 139.1 (dd, J = 16.0, 2.4 Hz, phosphinine CH), 132.8 (dd, J = 28.8, 10.4 Hz, *ipso*-Ph C), 131.5 (d, J = 12.8 Hz, PPh_2), 130.0 (d, J = 1.6 Hz, PPh_2), 128.8 (d, J = 9.6 Hz, PPh_2), 128.3-127.5 (m, phosphinine CH and C_6D_6 overlapping), 21.4 (s, 3-*H*); ^{31}P NMR (162 MHz, C_6D_6): δ = 222.7 (d, $^2J_{PP}$ = 71.1 Hz, 1-*P*), 20.0 (d, $^2J_{PP}$ = 71.1 Hz, 2-*P*); HRMS (ASAP/ QTof) m/z Calc. for $C_{22}H_{17}MoO_4P_2$: 504.9661 $[M+H]^+$; Found 504.9666; FTIR (ATR): ν(cm^{-1}) 1867 (CO), 1910 (CO), 2017 (CO); Anal. Calc. for $C_{22}H_{16}MoO_4P_2$: C 52.59, H 3.21; Found: C 52.46, H 3.17.

X-ray crystallography

Single crystals of the samples were covered in inert oil and placed under the cold stream of a Bruker X8 APEXII four-circle diffractometer cooled except for **4,** data for which were collected by the EPSRC National Crystallography Service on a XtaLAB AFC12 (RCD3) Kappa single diffractometer. Exposures were collected using Mo Kα radiation (λ = 0.71073). Indexing, data collection and absorption correction were performed using the APEXII suite of programs.[85] Structures were solved using direct or Patterson methods (SHELXS or SHELXT)[86] and refined by full-matrix least-squares (SHELXL)[86] interfaced with the programme OLEX2[87] (Table S1).

There was a disordered CH_2Cl_2 solvate molecule in **8** that was successfully modelled over two positions. CCDC deposition numbers: 1584358-1584363.

Supporting Information

The Supporting information contains spectroscopic data for **2**, **2.BH$_3$** and **3** – **7**, additional crystallographic information, further details on the catalysis, reactivity studies of proligand **1** and complex **3** with MAO and additional computational details.

Author information

Corresponding Authors

*E-mail: s.mansell@hw.ac.uk

*E-mail: martin.hanton@eu.sasol.com.

*E-mail: natalie.fey@bristol.ac.uk

Author Contributions

The manuscript was written through contributions of all authors. All authors have given approval to the final version of the manuscript. RJN and AS contributed equally to this work.

Notes

The authors declare no competing financial interest.

Acknowledgements

The authors would like to thank Sasol Technology for permission to publish this work, and the EPSRC UK National Mass Spectrometry Facility at Swansea University and the EPSRC UK

National Crystallography Service at the University of Southampton for assistance with sample analysis. Financial support is gratefully acknowledged from the EPSRC (DTP studentship to RJN), the Royal Society (Research grant: RG130436) and Heriot-Watt University as well as the UK Catalysis Hub Consortium (funded by EPSRC grants EP/K014706/2, EP/K014668/1, EP/K014854/1, EP/K014714/1 and EP/M013219/1) for providing travel funding to SMM and RJN.

References

1. Fernelius, C. W.; Wittcoff, H.; Varnerin, R. E., Ethylene: The organic chemical industry's most important building block. *J. Chem. Educ.* **1979,** *56*, 385-387.
2. van Leeuwen, P. W. N. M.; Clément, N. D.; Tschan, M. J. L., New processes for the selective production of 1-octene. *Coord. Chem. Rev.* **2011,** *255*, 1499-1517.
3. Keim, W., Oligomerization of Ethylene to α-Olefins: Discovery and Development of the Shell Higher Olefin Process (SHOP). *Angew. Chem., Int. Ed. Engl.* **2013,** *52*, 12492-12496.
4. Forestière, A.; Olivier-Bourbigou, H.; Saussine, L., Oligomerization of Monoolefins by Homogeneous Catalysts. *Oil & Gas Science and Technology - Rev. IFP* **2009,** *64*, 649-667.
5. McGuinness, D. S., Olefin Oligomerization via Metallacycles: Dimerization, Trimerization, Tetramerization, and Beyond. *Chem. Rev.* **2011,** *111*, 2321-2341.
6. Dixon, J. T.; Green, M. J.; Hess, F. M.; Morgan, D. H., Advances in selective ethylene trimerisation – a critical overview. *J. Organomet. Chem.* **2004,** *689*, 3641-3668.
7. Breuil, P.-A. R.; Magna, L.; Olivier-Bourbigou, H., Role of Homogeneous Catalysis in Oligomerization of Olefins : Focus on Selected Examples Based on Group 4 to Group 10 Transition Metal Complexes. *Catal. Lett.* **2015,** *145*, 173-192.
8. Wass, D. F., Chromium-catalysed ethene trimerisation and tetramerisation-breaking the rules in olefin oligomerisation. *Dalton Trans.* **2007**, 816-819.
9. Agapie, T., Selective ethylene oligomerization: Recent advances in chromium catalysis and mechanistic investigations. *Coord. Chem. Rev.* **2011,** *255*, 861-880.
10. Alferov, K. A.; Belov, G. P.; Meng, Y., Chromium catalysts for selective ethylene oligomerization to 1-hexene and 1-octene: Recent results. *Appl. Catal., A* **2017,** *542*, 71-124.
11. Overett, M. J.; Blann, K.; Bollmann, A.; Dixon, J. T.; Haasbroek, D.; Killian, E.; Maumela, H.; McGuinness, D. S.; Morgan, D. H., Mechanistic Investigations of the Ethylene Tetramerisation Reaction. *J. Am. Chem. Soc.* **2005,** *127*, 10723-10730.
12. Makume, B. F.; Maumela, M. C.; Holzapfel, C. W.; Dixon, J. T., Homo- and heteroditopic sulfur-based bidentate ligands towards selective ethylene oligomerisation: The critical influence of ligand structure on product profile. *Appl. Catal., A* **2017,** *542*, 262-270.
13. Britovsek, G. J. P.; McGuinness, D. S., A DFT Mechanistic Study on Ethylene Tri- and Tetramerization with Cr/PNP Catalysts: Single versus Double Insertion Pathways. *Chem.-Eur. J.* **2016,** *22*, 16891-16896.

14. Britovsek, G. J. P.; McGuinness, D. S.; Wierenga, T. S.; Young, C. T., Single- and Double-Coordination Mechanism in Ethylene Tri- and Tetramerization with Cr/PNP Catalysts. *ACS Catal.* **2015,** *5*, 4152-4166.
15. Suttil, J. A.; Wasserscheid, P.; McGuinness, D. S.; Gardiner, M. G.; Evans, S. J., A survey of pendant donor-functionalised (N,O) phosphine ligands for Cr-catalysed ethylene tri- and tetramerisation. *Catal. Sci. Tech.* **2014,** *4*, 2574-2588.
16. Mansell, S. M., Catalytic applications of small bite-angle diphosphorus ligands with single-atom linkers. *Dalton Trans.* **2017,** *46*, 15157-15174.
17. Carter, A.; Cohen, S. A.; Cooley, N. A.; Murphy, A.; Scutt, J.; Wass, D. F., High activity ethylene trimerisation catalysts based on diphosphine ligands. *Chem. Commun.* **2002**, 858-859.
18. Wass, D. F., BP Chemicals Ltd: 2002; p WO 02/04119.
19. Bollmann, A.; Blann, K.; Dixon, J. T.; Hess, F. M.; Killian, E.; Maumela, H.; McGuinness, D. S.; Morgan, D. H.; Neveling, A.; Otto, S.; Overett, M.; Slawin, A. M. Z.; Wasserscheid, P.; Kuhlmann, S., Ethylene Tetramerization: A New Route to Produce 1-Octene in Exceptionally High Selectivities. *J. Am. Chem. Soc.* **2004,** *126*, 14712-14713.
20. Blann, K.; Bollmann, A.; Dixon, J. T.; Neveling, A.; Morgan, D. H.; Maumela, H.; Killian, E.; Hess, F.; Otto, S.; Pepler, L.; Mahomed, H.; Overett, M., Sasol Technology: 2004; p WO Patent 04056479A1.
21. Agapie, T.; Schofer, S. J.; Labinger, J. A.; Bercaw, J. E., Mechanistic Studies of the Ethylene Trimerization Reaction with Chromium−Diphosphine Catalysts: Experimental Evidence for a Mechanism Involving Metallacyclic Intermediates. *J. Am. Chem. Soc.* **2004,** *126*, 1304-1305.
22. Agapie, T.; Labinger, J. A.; Bercaw, J. E., Mechanistic Studies of Olefin and Alkyne Trimerization with Chromium Catalysts: Deuterium Labeling and Studies of Regiochemistry Using a Model Chromacyclopentane Complex. *J. Am. Chem. Soc.* **2007,** *129*, 14281-14295.
23. Do, L. H.; Labinger, J. A.; Bercaw, J. E., Mechanistic Studies of Ethylene and α-Olefin Co-Oligomerization Catalyzed by Chromium–PNP Complexes. *Organometallics* **2012,** *31*, 5143-5149.
24. Stennett, T. E.; Haddow, M. F.; Wass, D. F., Avoiding MAO: Alternative Activation Methods in Selective Ethylene Oligomerization. *Organometallics* **2012,** *31*, 6960-6965.
25. Hirscher, N. A.; Agapie, T., Stoichiometrically Activated Catalysts for Ethylene Tetramerization using Diphosphinoamine-Ligated Cr Tris(hydrocarbyl) Complexes. *Organometallics* **2017,** *36*, 4107-4110.
26. Do, L. H.; Labinger, J. A.; Bercaw, J. E., Spectral Studies of a Cr(PNP)–MAO System for Selective Ethylene Trimerization Catalysis: Searching for the Active Species. *ACS Catal.* **2013,** *3*, 2582-2585.
27. Overett, M. J.; Blann, K.; Bollmann, A.; de Villiers, R.; Dixon, J. T.; Killian, E.; Maumela, M. C.; Maumela, H.; McGuinness, D. S.; Morgan, D. H.; Rucklidge, A.; Slawin, A. M. Z., Carbon-bridged diphosphine ligands for chromium-catalysed ethylene tetramerisation and trimerisation reactions. *J. Mol. Catal. A: Chem.* **2008,** *283*, 114-119.
28. Dulai, A.; Bod, H.; Hanton, M. J.; Smith, D. M.; Downing, S.; Mansell, S. M.; Wass, D. F., C-Substituted Bis(diphenylphosphino)methane-Type Ligands for Chromium-Catalyzed Selective Ethylene Oligomerization Reactions. *Organometallics* **2009,** *28*, 4613-4616.
29. Zhang, J.; Wang, X.; Zhang, X.; Wu, W.; Zhang, G.; Xu, S.; Shi, M., Switchable Ethylene Tri-/Tetramerization with High Activity: Subtle Effect Presented by Backbone-Substituent of Carbon-Bridged Diphosphine Ligands. *ACS Catal.* **2013,** *3*, 2311-2317.

30. Müller, C.; Vogt, D., Phosphinines as ligands in homogeneous catalysis: recent developments, concepts and perspectives. *Dalton Trans.* **2007**, 5505-5523.
31. Muller, C.; Vogt, D., Recent developments in the chemistry of donor-functionalized phosphinines. *C. R. Chim.* **2010,** *13*, 1127-1143.
32. Muller, C.; Vogt, D., *Phosphinine-Based Ligands in Homogeneous Catalysis: State of the Art and Future Perspectives*. 2011; Vol. 37, p 151-181.
33. Weber, L., Phosphorus Heterocycles: From Laboratory Curiosities to Ligands in Highly Efficient Catalysts. *Angew. Chem., Int. Ed. Engl.* **2002,** *41*, 563-572.
34. DiMauro, E. F.; Kozlowski, M. C., Phosphabenzenes as electron withdrawing phosphine ligands in catalysis. *J. Chem. Soc., Perkin Trans. 1* **2002**, 439-444.
35. Muller, C.; Broeckx, L. E. E.; de Krom, I.; Weemers, J. J. M., Developments in the Coordination Chemistry of Phosphinines. *Eur. J. Inorg. Chem.* **2013**, 187-202.
36. Floch, P. L., Phosphaalkene, phospholyl and phosphinine ligands: New tools in coordination chemistry and catalysis. *Coord. Chem. Rev.* **2006,** *250*, 627-681.
37. Newland, R. J.; Wyatt, M. F.; Wingad, R. L.; Mansell, S. M., A ruthenium(II) bis(phosphinophosphinine) complex as a precatalyst for transfer-hydrogenation and hydrogen-borrowing reactions. *Dalton Trans.* **2017,** *46*, 6172-6176.
38. Radcliffe, J. E.; Batsanov, A. S.; Smith, D. M.; Scott, J. A.; Dyer, P. W.; Hanton, M. J., Phosphanyl Methanimine (PCN) Ligands for the Selective Trimerization/Tetramerization of Ethylene with Chromium. *ACS Catal.* **2015,** *5*, 7095-7098.
39. Blug, M.; Piechaczyk, O.; Fustier, M.; Mézailles, N.; Le Floch, P., Protodesilylation of 2,6-Disubstituted Silyphosphinines. Experimental and Theoretical Study. *J. Org. Chem.* **2008,** *73*, 3258-3261.
40. Müller, C.; Habicht, M.; Wossidlo, F.; Bens, T.; Pidko, E., 2-(Trimethylsilyl)-λ3-Phosphinine: Synthesis, Coordination Chemistry and Reactivity. *Chem.-Eur. J.* **2018,** *24*, 944–952.
41. Ferro, V. R.; Omar, S.; Gonzalez-Jonte, R. H.; de la Vega, J. M. G., The sigma-donating and pi-accepting properties of ortho-Si(CH3)(3) phosphinine macrocycles. *Heteroat. Chem.* **2003,** *14*, 160-169.
42. Le Floch, P.; Carmichael, D.; Ricard, L.; Mathey, F., Palladium(0)-catalyzed functionalization of bromophosphinines. *J. Am. Chem. Soc.* **1993,** *115*, 10665-10670.
43. Kühl, O., Predicting the net donating ability of phosphines—do we need sophisticated theoretical methods? *Coord. Chem. Rev.* **2005,** *249*, 693-704.
44. Tolman, C. A., Steric effects of phosphorus ligands in organometallic chemistry and homogeneous catalysis. *Chem. Rev.* **1977,** *77*, 313-348.
45. van der Slot, S. C.; Duran, J.; Luten, J.; Kamer, P. C. J.; van Leeuwen, P. W. N. M., Rhodium-Catalyzed Hydroformylation and Deuterioformylation with Pyrrolyl-Based Phosphorus Amidite Ligands: Influence of Electronic Ligand Properties. *Organometallics* **2002,** *21*, 3873-3883.
46. Anton, D. R.; Crabtree, R. H., Metalation-resistant ligands: some properties of dibenzocyclooctatetraene complexes of molybdenum, rhodium and iridium. *Organometallics* **1983,** *2*, 621-627.
47. Märkl, G.; Dörges, C.; Riedl, T.; Klärner, F. G.; Lodwig, C., (4+2)-Cycloadditionen von 1,3λ3-azaphosphininen mit alkinylphosphanen bei hohen drucken. *Tetrahedron Lett.* **1990,** *31*, 4589-4592.

48. Mézailles, N.; Le Floch, P.; Waschbüsch, K.; Ricard, L.; Mathey, F.; Kubiak, C. P., Synthesis and X-ray crystal structures of dimeric nickel(0) and tetrameric copper(I) iodide complexes of 2-diphenylphosphino-3-methylphosphinine. *J. Organomet. Chem.* **1997,** *541*, 277-283.
49. Brèque, A.; Santini, C. C.; Mathey, F.; Fischer, J.; Mitschler, A., 4,5-Dimethyl-2-(2-pyridyl)phosphorin as a chelating ligand. Synthesis and x-ray crystal structure analysis of (4,5-dimethyl-2-(2-pyridyl)phosphorin)tetracarbonylchromium. *Inorg. Chem.* **1984,** *23*, 3463-3467.
50. Fronczek, F. R., *Private communication to CSD* **2014**.
51. Wong, G. W.; Harkreader, J. L.; Mebi, C. A.; Frost, B. J., Synthesis and Coordination Chemistry of a Novel Bidentate Phosphine: 6-(Diphenylphosphino)-1,3,5-triaza-7-phosphaadamantane (PTA-PPh2). *Inorg. Chem.* **2006,** *45*, 6748-6755.
52. Elschenbroich, C.; Voss, S.; Schiemann, O.; Lippek, A.; Harms, K., η1-Coordination of Phosphinine to Chromium, Molybdenum, and Tungsten,1. *Organometallics* **1998,** *17*, 4417-4424.
53. Waschbüch, K.; Le Floch, P.; Ricard, L.; Mathey, F., 2-Phosphanylphosphinines as Bridging Ligands for Dinuclear Transition Metal Carbonyls. *Chem. Ber.* **1997,** *130*, 843-849.
54. Le Floch, P.; Ricard, L.; Mathey, F., X-Ray crystal structure analysis and reactivity of (2-chlorophosphinine)pentacarbonyltungsten complexes. *Polyhedron* **1990,** *9*, 991-997.
55. Mao, Y.; Mathey, F., The Conversion of Furans into Phosphinines. *Chem.-Eur. J.* **2011,** *17*, 10745-10751.
56. Rhörig, U.; Mézailles, N.; Maigrot, N.; Ricard, L.; Mathey, F.; Le Floch, P., Syntheses of Phosphinine-Based Tripodal Ligands. *Eur. J. Inorg. Chem.* **2000,** *2000*, 2565-2571.
57. Rosa, P.; Ricard, L.; Le Floch, P.; Mathey, F.; Sini, G.; Eisenstein, O., Synthesis, Unusual Trigonal Prismatic Geometry, and Theoretical Study of the Homoleptic Tris-(2,2'-biphosphinine) Complexes of Chromium, Molybdenum, and Tungsten. *Inorg. Chem.* **1998,** *37*, 3154-3158.
58. Grim, S. O.; Briggs, W. L.; Barth, R. C.; Tolman, C. A.; Jesson, J. P., Unsymmetrical bis-phosphorus ligands. IV. Group VI metal carbonyl derivatives of diphenylphosphinomethyl and diphenylphosphinomethyl phosphinites, (C6H5)2P(CH2)nOP(C6H5)2, n = 1 or 2, and an unusual phosphorus chemical shift chelate effect. *Inorg. Chem.* **1974,** *13*, 1095-1100.
59. Märkl, G.; Lieb, F.; Merz, A., Elektrophile Reaktionen des 2,4,6-Triphenylphosphabenzols. *Angew. Chem., Int. Ed. Engl.* **1967,** *79*, 59-59.
60. Ashe, A. J.; Smith, T. W., The reaction of phosphabenzene, arsabenzene and stibabenzene with methyllithium. *Tetrahedron Lett.* **1977,** *18*, 407-410.
61. Bruce, M.; Meissner, G.; Weber, M.; Wiecko, J.; Müller, C., Lithium Salts of 2,4,6-Triaryl-λ4-phosphinine Anions – A Comparison Study. *Eur. J. Inorg. Chem.* **2014,** *2014*, 1719-1726.
62. Moores, A.; Ricard, L.; Le Floch, P.; Mézailles, N., First X-ray Crystal Study and DFT Calculations of Anionic λ4-Phosphinines. *Organometallics* **2003,** *22*, 1960-1966.
63. Dochnahl, M.; Doux, M.; Faillard, E.; Ricard, L.; Le Floch, P., A New Mixed P,S-Bidentate Ligand Featuring a λ4-Phosphinine Anion and a Phosphanyl Sulfide Group − Synthesis, X-ray Crystal Structures and Catalytic Properties of Its Chloro(cymene)ruthenium and Allylpalladium Complexes. *Eur. J. Inorg. Chem.* **2005,** *2005*, 125-134.
64. Doux, M.; Bouet, C.; Mézailles, N.; Ricard, L.; Le Floch, P., Synthesis and Molecular Structure of a Palladium Complex Containing a λ5-Phosphinine-Based SPS Pincer Ligand. *Organometallics* **2002,** *21*, 2785-2788.

65. Doux, M.; Mezailles, N.; Melaimi, M.; Ricard, L.; Le Floch, P., A [sigma]4, [small lambda]5-phosphinine palladium complex: a new type of phosphorus ligand and catalyst. Application to the Pd-catalyzed formation of arylboronic esters. *Chem. Commun.* **2002**, 1566-1567.
66. Doux, M.; Mézailles, N.; Ricard, L.; Le Floch, P., Group 10 Metal Complexes of SPS-Based Pincer Ligands: Syntheses, X-ray Structures, and DFT Calculations. *Eur. J. Inorg. Chem.* **2003,** *2003*, 3878-3894.
67. Doux, M.; Ricard, L.; Le Floch, P.; Jean, Y., Addition of H2 on (Sulfur, Phosphorus, Sulfur)-Pincer-Based Rhodium(I), Iridium(I), Palladium(II), and Platinum(II) Complexes: Reactivity and Regioselectivity. *Organometallics* **2006,** *25*, 1101-1111.
68. Moores, A.; Mézailles, N.; Ricard, L.; Jean, Y.; le Floch, P., η2-Palladium and Platinum(II) Complexes of a λ4-Phosphinine Anion: Syntheses, X-ray Crystal Structures, and DFT Calculations. *Organometallics* **2004,** *23*, 2870-2875.
69. Moores, A.; Mézailles, N.; Ricard, L.; Le Floch, P., η5-Rhodium(I) Complexes of a λ4-Phosphinine Anion: Syntheses, X-ray Crystal Structures, and Application in the Catalyzed Hydroformylation of Olefins. *Organometallics* **2005,** *24*, 508-513.
70. Hoidn, C. M.; Wolf, R., Reaction of a 2,4,6-triphenylphosphinine ferrate anion with electrophiles: a new route to phosphacyclohexadienyl complexes. *Dalton Trans.* **2016,** *45*, 8875-8884.
71. Lehmkuhl, H.; Paul, R.; Krüger, C.; Tsay, Y.-H.; Benn, R.; Mynott, R., 1,2,4,6-Tetraorganophosphorinylnickel-Komplexe. *Liebigs Ann. Chem.* **1981,** *1981*, 1147-1161.
72. Fey, N.; Orpen, A. G.; Harvey, J. N., Building ligand knowledge bases for organometallic chemistry: Computational description of phosphorus(III)-donor ligands and the metal–phosphorus bond. *Coord. Chem. Rev.* **2009,** *253*, 704-722.
73. Gusev, D. G., Donor Properties of a Series of Two-Electron Ligands. *Organometallics* **2009,** *28*, 763-770.
74. Jover, J.; Fey, N., The Computational Road to Better Catalysts. *Chem. Asian J.* **2014,** *9*, 1714-1723.
75. Perrin, L.; Clot, E.; Eisenstein, O.; Loch, J.; Crabtree, R. H., Computed Ligand Electronic Parameters from Quantum Chemistry and Their Relation to Tolman Parameters, Lever Parameters, and Hammett Constants. *Inorg. Chem.* **2001,** *40*, 5806-5811.
76. Fey, N., Lost in chemical space? Maps to support organometallic catalysis. *Chem. Cent. J.* **2015,** *9*, 38.
77. Fey, N.; Garland, M.; Hopewell, J. P.; McMullin, C. L.; Mastroianni, S.; Orpen, A. G.; Pringle, P. G., Stable Fluorophosphines: Predicted and Realized Ligands for Catalysis. *Angew. Chem., Int. Ed. Engl.* **2012,** *51*, 118-122.
78. Fey, N.; Tsipis, A. C.; Harris, S. E.; Harvey, J. N.; Orpen, A. G.; Mansson, R. A., Development of a Ligand Knowledge Base, Part 1: Computational Descriptors for Phosphorus Donor Ligands. *Chem.-Eur. J.* **2006,** *12*, 291-302.
79. Jover, J.; Fey, N.; Harvey, J. N.; Lloyd-Jones, G. C.; Orpen, A. G.; Owen-Smith, G. J. J.; Murray, P.; Hose, D. R. J.; Osborne, R.; Purdie, M., Expansion of the Ligand Knowledge Base for Chelating P,P-Donor Ligands (LKB-PP). *Organometallics* **2012,** *31*, 5302-5306.
80. Jover, J.; Fey, N.; Harvey, J. N.; Lloyd-Jones, G. C.; Orpen, A. G.; Owen-Smith, G. J. J.; Murray, P.; Hose, D. R. J.; Osborne, R.; Purdie, M., Expansion of the Ligand Knowledge Base for Monodentate P-Donor Ligands (LKB-P). *Organometallics* **2010,** *29*, 6245-6258.

81. Fey, N.; Harvey, J. N.; Lloyd-Jones, G. C.; Murray, P.; Orpen, A. G.; Osborne, R.; Purdie, M., Computational Descriptors for Chelating P,P- and P,N-Donor Ligands1. *Organometallics* **2008,** *27*, 1372-1383.
82. Fey, N.; Papadouli, S.; Pringle, P. G.; Ficks, A.; Fleming, J. T.; Higham, L. J.; Wallis, J. F.; Carmichael, D.; Mézailles, N.; Müller, C., Setting P-Donor Ligands into Context: An Application of the Ligand Knowledge Base (LKB) Approach. *Phosphorus, Sulfur Silicon Relat. Elem.* **2015,** *190*, 706-714.
83. Bennett, M. A.; Wilkinson, G.; Pratt, L., Transition-metal complexes of 7-membered ring systems. 4. Proton resonance spectra of cycloheptatriene complexes of group vi metals. *J. Chem. Soc.* **1961**, 2037-2044.
84. Shupp, J. P.; Kinne, A. S.; Arman, H. D.; Tonzetich, Z. J., Synthesis and Characterization of Molybdenum(0) and Tungsten(0) Complexes of Tetramethylthiourea: Single-Source Precursors for MoS2 and WS2. *Organometallics* **2014,** *33*, 5238-5245.
85. *Bruker AXS APEX2, version 2009-5*, version 2009-5; Bruker AXS Inc.: Madison,Wisconsin, USA, 2009.
86. Sheldrick, G. M., A short history of SHELX. *Acta Crystallogr., Sect. A: Found. Crystallogr.* **2008,** *64*, 112-122.
87. Dolomanov, O. V.; Bourhis, L. J.; Gildea, R. J.; Howard, J. A. K.; Puschmann, H., OLEX2: a complete structure solution, refinement and analysis program. *J. Appl. Crystallogr.* **2009,** *42*, 339-341.